# Intelligent Vehicle Power Control based on Prediction of Road Type and Traffic Congestions

Jungme Park, ZhiHang Chen, Ming Kuang, *Member, IEEE*, Abul Masrur, Senior *Member, IEEE*, Anthony Phillips, *Member, IEEE*, Yi L. Murphey, Senior *Member, IEEE*

*Abstract*—This paper presents a machine learning approach to the efficient vehicle power management and an intelligent power controller (IPC) that applies the learnt knowledge about the optimal power control parameters specific to road types and traffic congestion levels to online vehicle power control. The IPC uses a neural network for online prediction of roadway types and traffic congestion levels. The IPC and the prediction model have been implemented in a conventional (non-hybrid) vehicle model for online vehicle power control in a simulation program. The benefits of the IPC combined with the predicted drive cycle are demonstrated through simulation. Experiment results show that the IPC gives close to optimal performances.

## I. Introduction

VEHICLE power management has been an active research area in the past decade, and has intensified recently by the emergence of hybrid electric vehicle technologies. Most of these approaches were developed based on mathematical models or human expertise, and knowledge derived from simulation data. The application of optimal control theory to power distribution and management has been the most popular approach, which includes linear programming [1], optimal control [2], and, especially, dynamic programming (DP) [3, 4, 5]. In general, these techniques do not offer an on-line solution, because they assume that the future driving cycle is entirely known. However these results can be used as a benchmark for the performance of power control strategies. More recently various techniques for deriving effective online control rules based on the results generated by offline DP and Quadratic Programming (QP) [3, 6]. However few attempts have been made to explore the optimization of vehicle power management with the knowledge of road type and traffic congestions, which is the main contribution of this paper. A comprehensive overview of intelligent systems approaches for vehicle power management can be found in [7].

Driving patterns exhibited in a real world driver are the product of the instantaneous decisions of the driver to cope with the (physical) driving environment. Research has shown that driving style and environment have strong influence over fuel consumption and emissions [8,9]. Specifically road type and traffic conditions, driving trend, driving style, and vehicle operation modes have various degrees of impacts on vehicle fuel consumptions. However most of the existing vehicle power control approaches do not incorporate the knowledge about driving patterns into their vehicle power management strategies.

Our research focuses on developing a machine learning strategy to learn about the optimal control parameters for all 11 standard facility specific drive cycles proposed in [10] and an intelligent online power controller (IPC) that applies the learnt optimal control parameters to online vehicle power management based on a neural network system trained to predict the current road type and traffic congestion level.

This paper is organized as follows. Section II introduces the intelligent vehicle power management and machine learning algorithms. Section III introduces the online control strategy and the performances of IPC. Section IV is the conclusion.

## II. Intelligent Power Control in a Conventional Vehicle System

### A. A conventional vehicle model for fuel consumption optimization

Figure 1 shows the interaction between the proposed Intelligent Power Controller (IPC) and a conventional vehicle system. During a drive cycle, the IPC calls the neural network, NN_RT&TC, to predict the current road type and traffic congestion (RT&TC) level. The IPC uses the output, R[i], $1 \le i \le 11$, from NN_RT&TC to retrieve the knowledge about the optimal power control parameters applicable to the predicted road type and traffic congestion level, applies the knowledge and the current vehicle state, which is represented by the current vehicle speed v(t), driver power demand $P_d(t)$, electrical load $P_l(t)$ and SOC of the battery, to calculating the electric power setpoint, $P_s$, for the battery controller, and the setpoint, $P_e$, for the alternator, a feed forward torque compensation to the engine controller. $P_s$ represents the power actually to be charged ($P_s > 0$) or discharged ($P_s < 0$) from the battery and is set by the IPC with the aim of minimizing fuel consumption. The optimal engine power $P_{eng}$, calculated based optimal setpoint of $P_s$, is used to find the optimal feed forward torque compensation through the engine fuel efficiency map. The functional relationship between $P_{eng}$ and $P_s$ are shown as follows:

This work was supported in part by the state of Michigan under 21st Jobs Fund.

JungMe Park, ZhiHang Chen and Yi L. Murphey are with the Department of Electrical and Computer Engineering, University of Michigan-Dearborn (phone: 313-593-5028, fax: 313-583-6336, email: yilu@umich.edu)

Ming Kuang and Anthony Phillips are with Ford Motor Company, Dearborn, MI, USA.

M.A. Masrur is with the US Army RDECOM-TARDEC, Warren, MI 49307.

# Report Documentation Page

*Form Approved*
*OMB No. 0704-0188*



| | | |
|---|---|---|
| 1. REPORT DATE<br>**21 SEP 2008** | 2. REPORT TYPE<br>**N/A** | 3. DATES COVERED<br>**-** |

| | |
|---|---|
| 4. TITLE AND SUBTITLE<br>**Intelligent Vehicle Power Control Based on Prediction of Road Type and Traffic Congestions** | 5a. CONTRACT NUMBER<br>5b. GRANT NUMBER<br>5c. PROGRAM ELEMENT NUMBER |
| 6. AUTHOR(S)<br>**Jungme Park; ZhiHang Chen; Ming Kuang; Abul Masrur; Anthony Philips; Yi L. Murphey** | 5d. PROJECT NUMBER<br>5e. TASK NUMBER<br>5f. WORK UNIT NUMBER |
| 7. PERFORMING ORGANIZATION NAME(S) AND ADDRESS(ES)<br>**US Army RDECOM-TARDEC 6501 E 11 Mile Rd Warren, MI 48397-5000** | 8. PERFORMING ORGANIZATION REPORT NUMBER<br>**18911** |
| 9. SPONSORING/MONITORING AGENCY NAME(S) AND ADDRESS(ES) | 10. SPONSOR/MONITOR'S ACRONYM(S)<br>**TACOM/TARDEC**<br>11. SPONSOR/MONITOR'S REPORT NUMBER(S)<br>**18911** |

12. DISTRIBUTION/AVAILABILITY STATEMENT
**Approved for public release, distribution unlimited**

13. SUPPLEMENTARY NOTES
**Appears in: Vehicular Technology Conference, 2008, VTC 2008-Fall, IEEE 68th. Publication Date 21-24 Sept. 2008. On page(s): 1-5 Location: Calgary, Canada,, The original document contains color images.**

14. ABSTRACT

15. SUBJECT TERMS

| 16. SECURITY CLASSIFICATION OF: | | | 17. LIMITATION OF ABSTRACT | 18. NUMBER OF PAGES | 19a. NAME OF RESPONSIBLE PERSON |
|---|---|---|---|---|---|
| a. REPORT<br>**unclassified** | b. ABSTRACT<br>**unclassified** | c. THIS PAGE<br>**unclassified** | **SAR** | **5** | |

$$P_{eng} = P_d + G(P_e, \omega_e),\ P_e = P_l + P_b\ ,\ P_b = P_s + P\_Loss_{bat}\ (P_s, E_s, T),$$

where $G(P_e, \omega_e)$ is the efficiency map of converting mechanical to electrical power in the vehicle system. $P\_Loss_{bat}$, representing the power losses in the battery, is a function of $P_s$, $E_s$ (energy level in the battery), and T(the temperature). To simplify the problem, we ignore the influence of $E_s$ and T, and model the power loss, $P\_Loss_{bat}$, during charging and discharging as follows:

$$P_b = \left\{ \begin{array}{ll} \frac{1}{\eta_{charge}} * P_s & if\ P_s > 0 \\ \eta_{discharge} * P_s & if\ P_s < 0 \end{array} \right\}.$$

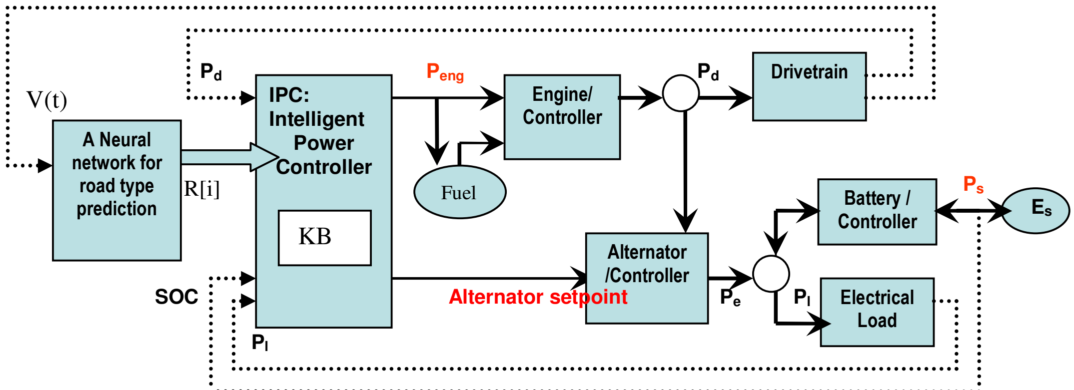


$P_{eng}$ – engine power demand , Ps: power charged to or discharged from battery
$P_d$ - driver power demand, $P_e$: electrical power at alternator
$P_l$ – electrical load , V(t): vehicle speed at time t

Figure 1. Intelligent power controller in a vehicle system.

TABLE I.
STATISTICS OF 11 FACILITY SPECIFIC DRIVING CYCLES [10]

| Drive Cycles | $V_{avg}$ (mph) | $V_{max}$ (mph) | $A_{max}$ (mph/s$^2$) | Length (sec) |
|---|---|---|---|---|
| **Freeway LOS A: R[1]** | 67.79 | 79.52 | 2.3 | 399 |
| **Freeway LOS B: R[2]** | 66.91 | 78.34 | 2.9 | 366 |
| **Freeway LOS C: R[3]** | 66.54 | 78.74 | 3.4 | 448 |
| **Freeway LOS D: R[4]** | 65.25 | 77.56 | 2.9 | 433 |
| **Freeway LOS E: R[5]** | 57.2 | 74.43 | 4.0 | 471 |
| **Freeway LOS F: R[6]** | 32.63 | 63.85 | 4.0 | 536 |
| **Freeway Ramps: R[7]** | 34.6 | 60.2 | 5.7 | 266 |
| **Arterials LOS A-B: R[8]** | 24.8 | 58.9 | 5.0 | 737 |
| **Arterials LOS C-D: R[9]** | 19.2 | 49.5 | 5.7 | 629 |
| **Arterials LOS E-F: R[10]** | 11.6 | 39.9 | 5.8 | 504 |
| **Local Roadways: R[11]** | 12.9 | 38.3 | 3.7 | 525 |

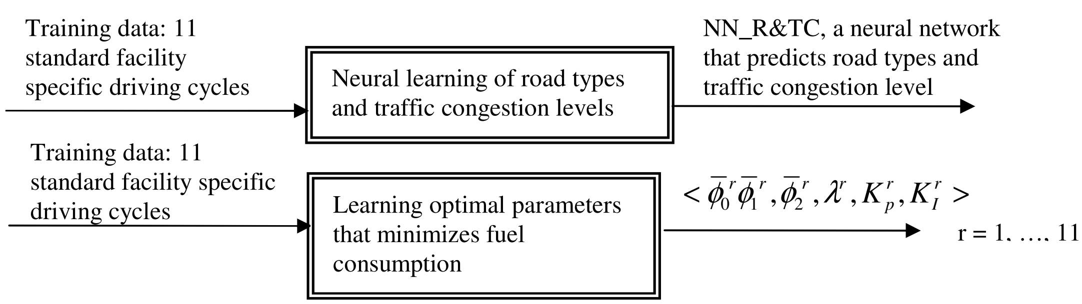


Figure 2: Machine learning processes.

The fuel optimization problem is modeled as a multistep decision problem using a quadratic function of $P_s$

$$\underset{P_s}{Min}\, J = \sum_{k=0}^{n} \min_{P_s} \gamma(P_s(k),k) \approx \sum_{k=0}^{n} \min_{P_s} \frac{1}{2}\varphi_2 P_s^2(k) + \varphi_1(k) P_s(k) + \varphi_0(k) \cdot$$

where $\overline{P}_s$ contains the optimal setting of $P_s(k)$, for k = 0, …, n, n is the number of time intervals in a given driving cycle. The quadratic function of the fuel rate is solved by the following computational steps:

step 1: Minimizing the following Lagrange function of with respect to $P_s$ and $\lambda$:

$$L(Ps(1),...,Ps(N),\lambda) = \sum_{k=1}^{N}\{\varphi_2(k)Ps(k)^2 + \varphi_1(k)Ps(k)\} + \phi_0(k) - \lambda\sum_{k=1}^{N} Ps(k)$$

Step 2: Taking the partial derivatives of Lagrange function L with respect to $P_s$ (k), k=1,…,N and $\lambda$ respectively, and setting the equations to 0, we have
optimal battery setting:

$$P_s(k) = \frac{\lambda - \varphi_1(k)}{2\varphi_2(k)}$$

Step 3: Using the PI-type controller such that the $E_s$ value of the battery should be kept near a nominal value of the initial $E_s$ of a battery at the beginning of the driving cycle:[6]

$$\lambda(k) = \lambda_0 + Kp(Es(1) - Es(k)) + Ki\sum_{t=1}^{k}(Es(1) - Es(t))\Delta t \cdot$$

The optimal parameters, $\varphi_0(k)$, $\varphi_1(k)$, $\varphi_2(k)$, $\lambda_0$ and the $K_p$ and $K_i$ are obtained by the machine learning algorithm described in the next subsection.

### *B. Machine learning of minimizing fuel consumption*

We model the road environment of a driving trip as a sequence of different road types such as local, freeway, arterial/collector, etc. augmented with different traffic congestion levels. We use the set of 11 standard facility specific(FS) drive cycles presented in [10, 11] to represent passenger car and light truck operations over a range of facilities and congestion levels in urban areas. The 11 FS drive cycles are divided into four categories, freeway, freeway ramp, arterial, and local. The two categories, freeway and arterial are further divided into subcategories based on a qualitative measure called level of service (LOS) that describes operational conditions within a traffic stream based on speed and travel time, freedom to maneuver, traffic interruptions, comfort, and convenience [10]. For the convenience of description we label the 11 classes of roadway types and congestion level as R[1], …., R[11]. Table I shows the most recent definition of these road types[10] along with the labels we assigned.

We formulate the problem of optimal vehicle power management as follows. For a drive cycle DC(t), $t \in [0, t_e)$, where $t_e$ is the ending time of the drive cycle, at any given time t, the vehicle is on one of the 11 road types and traffic congestion levels, R[i], i = 1, …, 11, and the optimal power settings for R[i] should be applied to the vehicle power system during time interval [t, t+$\Delta t$ ).

Figure 2 shows the two major machine learning processes: training a neural network to predict road types and traffic congestion levels, and machine learning optimal power settings for all 11 FS drive cycles.

The algorithm for the machine learning of optimal parameters has the following computational steps:

Step 1. For each FS drive cycle, R[i], i = 1, …, 11, use the selected vehicle model to run the simulation program to generate step-by-step system state data: $P_d(k)$, $P_l(k)$, $\omega(k)$(engine speed), k=1, … , N.

Step 2. From the simulation results, generate a fuel rate matrix F_R($P_s(k)$, kl $\omega(k)$, $P_d(k)$, $P_l(k)$), where k is the discretized time step, $P_s(k)$ is the charge and discharge power within the system constraints[6] at time k for the given engine speed, $\omega(k)$, required drivetrain power $P_d(k)$, and the electric load power $P_l(k)$.

Step 3. At each time step k, the $k^{th}$ column of matrix F_R( *, k) is represented as a convex quadratic cost function of $P_s$. By using a regression method, we obtain coefficients $\varphi_2(k)$, $\varphi_1(k)$ and $\varphi_0(k)$, such that $\varphi_2(k)P_s^2(k) + \varphi_1(k)P_s(k) + \varphi_0(k) \approx$ F_R( *, k) with the best fit.

Step 4 From $\tilde{\varphi}_2^i$ and $\tilde{\varphi}_1^i$, the average values of the coefficients of, $\varphi_1(k)$ and $\varphi_2(k)$, we calculate the $K_p^i$ and $K_I^i$ using the following formulas[6] for the FS drive cycle R[i].

$$K_p^i = \tilde{\varphi}_2^i * 2 * 10^{-3}, \quad K_I^i = \tilde{\varphi}_2^i * 3.3 * 10^{-4} / \tilde{\varphi}_1^i.$$

We applied the above machine learning algorithm to the 11 FS drive cycles and the results are shown in Table II, which is used in online control as the knowledge base by IPC.

We developed a multi-layered, multi-class neural network, NN_RT&TC, for the prediction of the 11 road types and traffic congestion levels. The training data are obtained by segmenting and labeling all 11 drive cycles provided by [12]. For a window size, $\Delta w$, time step, $\Delta t$, and a given drive cycle DC(t) ($0 \le t \le t_e$), we extract a feature vector $\overline{x}$ from a segment DC[t-$\Delta w$, t], and NN_RT&TC takes $\overline{x}$ and predicts the road type and congestion level during the time interval [t, t+$\Delta t$ ).

Based on an in depth study on the neural network learning[13], the effective window size, time step and feature vector are found as follows: $\Delta w$ = 150 seconds, $\Delta t$ =3, a vector of the 14 features. The detail of the neural learning and prediction can be found in [13].

## III. ONLINE INTELLIGENT POWER CONTROL AND EXPERIMENTS

The neural network, NN_RT&TC, and the intelligent power controller, IPC, have been fully implemented in the PSAT simulation environment for online vehicle power control.

Table II. Optimal parameter settings generated by the machine learning algorithm for 11 standard FS drive cycles.

| Standard FS drive cycles | Avg of Quadratic Cost Function Coefficients | | lambda | PI Controller coefficient | |
|---|---|---|---|---|---|
| | $\tilde{\varphi}_2$ | $\tilde{\varphi}_1$ | $\lambda$ | $K_P$ | $K_I$ |
| Freeway LOS A | 0.0795 | 1.8602 | 1.4948 | $3.18e^{-4}$ | $1.59e^{-7}$ |
| Freeway LOS B | 0.0793 | 1.8520 | 1.1201 | $3.17e^{-4}$ | $1.59e^{-7}$ |
| Freeway LOS C | 0.0852 | 1.8721 | 1.1801 | $3.41e^{-4}$ | $1.70e^{-7}$ |
| Freeway LOS D | 0.0796 | 1.8594 | 1.1203 | $3.18e^{-4}$ | $1.59e^{-7}$ |
| Freeway LOS E | 0.0924 | 1.9994 | 1.9447 | $3.70e^{-4}$ | $1.85e^{-7}$ |
| Freeway LOS F | 0.1243 | 2.2200 | 2.3371 | $4.97e^{-4}$ | $2.49e^{-7}$ |
| Freeway Ramp | 0.1204 | 2.3206 | 2.1549 | $4.82e^{-4}$ | $2.41e^{-7}$ |
| Arterial LOS A_B | 0.0752 | 2.1012 | 2.1657 | $3.01e^{-4}$ | $1.50e^{-7}$ |
| Arterial LOS C_D | 0.0771 | 2.1728 | 2.1558 | $3.08e^{-4}$ | $1.54e^{-7}$ |
| Arterial LOS E_F | 0.0488 | 2.1363 | 2.2030 | $1.95e^{-4}$ | $9.77e^{-8}$ |
| Local Roadway | 0.0561 | 2.1045 | 2.2027 | $2.24e^{-4}$ | $1.12e^{-7}$ |

The computational steps of IPC are as follows:

Step 1. For a drive cycle DC[t], if t < $\Delta w$, use the startup setting points, otherwise go to Step 2.

Step 2. Call NN_RT&TC to predict the FS road type and traffic congestion level based on the vehicle speed history during time interval, [t-$\Delta w$, t). Let the output from NN_RT&TC be R[r].

Step 3. Retrieve from the knowledge base the optimal parameters, for FS road class R[r], $< \bar{\varphi}_1^r, \bar{\varphi}_2^r, \lambda^r, K_p^r, K_I^r >$.

Step4. Get vehicle state data at current time t, $P_d(t)$, $P_l(t)$, $\omega(t)$ and the SOC value at the last time step, SOC(t-1).

Step5. Calculate the battery energy level,

Es(t-1) = SOC(t-1) * Battery_Capacity

Step6. Calculate Fuel rate F_R (Ps(t), t) at time,t,

F_R (Ps(t), t| $P_d(t)$, $P_l(t)$, $\omega(t)$) , where

$$P_s\_\min(t) \le P_s(t) \le P_s\_\max(t)$$

Step 7. Calculate

$$\lambda(t) = \lambda_0 + Kp^r(Es(1) - Es(t-1)) + Ki^r \sum_{p=1}^{t-1}(Es(1) - Es(p))$$

where $\lambda_0$ is the $\lambda$ value of the initial FS road class in this drive cycle.

Step 8. Calculate :

$$P_s^o(t) = \arg\min_{Ps(t)}\{F\_R(P_s(t),t) - \lambda(t) * P_s(t)\}$$

,where $P_s\_\min(t) \le P_s(t) \le P_s\_\max(t)$ Ps(t)

$$P_{eng}(t) = P_d(t) + \eta_{alt\_eff}(P_L + \eta_{bat\_eff} P_s^0(t)),$$

where $\eta_{alt\_eff}$ and $\eta_{bat\_eff}$ are Alternator coefficient and Battery coefficient respectively.

We conducted the experiments on three drive cycles using a conventional vehicle model provided by [12]. The vehicle model used has a 95KW 1.9L Liter Spark Ignition engine [12], 5 gear manual transmission and a 12-14V 1.5 KW alternator, and a 66Ah/12V lead acid battery. Experimental results for three drive cycles, UDDS, LA92 and UNIF01, are shown in Figure 3 and Table III. The UDDS drive cycle represents driving conditions in an urban area with frequent stops, the LA92 drive cycle was constructed of segments of actual driving recording in Los Angeles, and the UNIF01 Cycle, developed for the California Air Resources Board [10], is a modified form of the LA92. For the purpose of comparison we have used off-line Dynamic Programming (DP) to find the optimal operating points [3, 6]. Since the DP algorithm requires the full knowledge of the entire driving cycle to optimize the power management strategy, it is not applicable to online control. However the results generated by DP can be used as a benchmark for the performance of power control strategies. In Figure 5, we show the battery state of charge (SOC) for three different drive cycles using three different vehicle power control algorithms. The red curves in the plots show the SOC when DP is used for optimal prediction and control (with the knowledge of full drive cycle). The green curves show the SOC generated using the existing control strategy in [12]. Finally, the blue curves show the results when the ***IPC*** prediction and control routine is used as described above.

It can be observed that the SOC curves generated by the ***IPC*** for all three drive cycles have similar behavior to the respective ones generated by the offline DP algorithm. The SOC curves generated by the controller in [12], on the other hand, are significantly different from the optimal curves.

Table III presents the performance comparisons with respect to fuel consumption. We use the fuel consumed by the simulation vehicle with the conventional power management controller in [12] as the baseline for comparison. For the UDDS and LA 92 drive cycles, the ***IPC*** gives almost the identical fuel consumption as the optimal (DP) controller. On the UNIF01 drive cycle, the ***IPC*** saved 2.68% fuel in comparison to the baseline controller in [12]. Clearly by combining a prediction of the roadway type and congestion level with the proposed intelligent power management strategy, we were able to realize a fuel economy improvement over the existing conventional vehicle power management strategy.

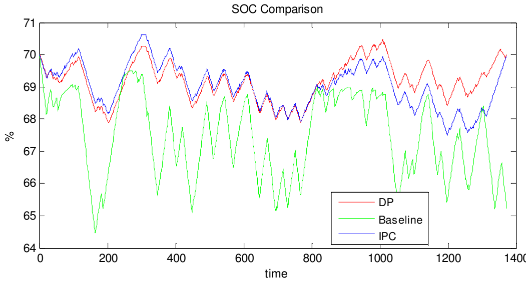


(a) SOC compensation during driving cycle UDDS

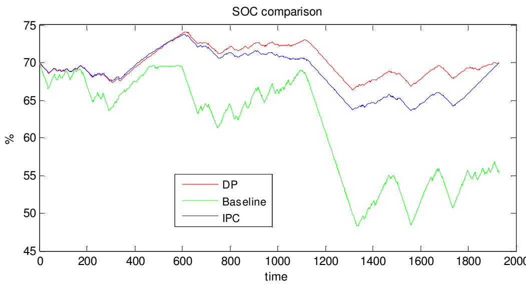


(b) SOC compensation during driving cycle UNIF01

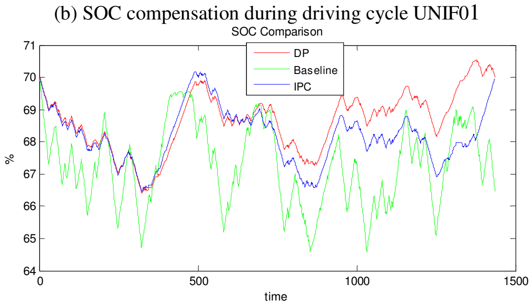


(c) SOC compensation during driving cycle LA92

Figure 3. SOC comparison on three driving cycles. The X axis represents time measured in seconds and the vertical represents the SOC measured in percentages.

TABLE III
Performance comparison on fuel consumption

| | Algorithm | Fuel Consumption (gram) | **Final SOC (%)** | Fuel Consumption After SOC correction 70% (gram) | **Saving From Baseline** |
|---|---|---|---|---|---|
| UDDS | Baseline | 701.1821 | 65.32% | 712.5429 | |
| | Off Line DP (optimal) | 700.2153 | 70.00% | 700.2153 | 1.7301% |
| | ***IPC*** | 700.1142 | 69.96% | 700.2207 | 1.7293% |
| ***UNIF01*** | Baseline | 1269.225 | 55.37% | 1304.799 | |
| | Off Line DP (optimal) | 1268.153 | 70.00% | 1268.153 | 2.8085% |
| | ***IPC*** | 1269.637 | 69.96% | 1269.743 | 2.6866% |
| **LA92** | Baseline | 980.191 | 66.56% | 988.63 | |
| | Off Line DP (optimal) | 973.428 | 70.00% | 973.42 | 1.538% |
| | ***IPC*** | 973.3181 | 69.96% | 973.42 | 1.538% |

## V. CONCLUSION

We have presented an intelligent vehicle power controller IPC developed for in-vehicle optimal power control based on the prediction of 11 different roadway types and traffic congestion levels.

The IPC uses the optimal control parameters generated for all 11 standard FS drive cycles and applies the appropriate optimal control parameters based on the road type predicted by the neural network NN_RT&TC to generate optimal power to be charged to or discharged from the battery. Our simulation results on the three drive cycles, UDDS, UNIF01 and LA 92 drive cycles show that IPC gives much better performance over the existing power management strategy in a conventional vehicle: for the UDDS and LA 92 drive cycles, the ***IPC*** gives almost the identical fuel consumption as the optimal (DP) controller; for the UNIF01 drive cycle, the ***IPC*** saved 2.68% fuel in comparison to the baseline controller. Currently we are applying the roadway prediction knowledge to a hybrid vehicle power management system. We anticipate more significant fuel reduction will be achieved in hybrid vehicle power systems.

## REFERENCES

[1] E. D. Tate and S. P. Boyd, "Finding ultimate limits of performance for hybrid electric vehicles,", SAE Paper-01-3099, 2000.

[2] S. Delprat, J. Lauber, T.M. Guerra, and J. Rimaux, "Control of a parallel hybrid powertrain: optimal control," *IEEE Trans. Veh. Technol.*, vol. 53, no. 3, pp. 872–881, May 2004.

[3] C.-C. Lin, H. Peng, J.W. Grizzle, and J.-M. Kang, "Power management strategy for a parallel hybrid electric truck," *IEEE Trans. Contr. Syst. Technol.*, vol. 11, no. 6, pp. 839–849, Nov. 2003.

[4] T. Hofman and R. van Druten, "Energy analysis of hybrid vehicle powertrains," in *Proc. IEEE Int. Symp. Veh. Power Propulsion*, Paris, France, Oct. 2004.

[5] I. Arsie, M. Graziosi, C. Pianese, G. Rizzo, and M. Sorrentino, "Optimization of supervisory control strategy for parallel hybrid vehicle with provisional load estimate," in *Proc. 7th Int. Symp. Adv. Vehicle Control(AVEC)*, Arnhem, The Netherlands, Aug. 2004.

[6] Koot, M.; Kessels, J.T.B.A.; de Jager, B.; Heemels, W.P.M.H.; van den Bosch, P.P.J.; Steinbuch, M., Energy management strategies for vehicular electric power systems, IEEE Transactions on Vehicular Technology, Volume 54, Issue 3, Page(s):771 – 782, May 2005.

[7] Yi L. Murphey, "Intelligent Vehicle Power Management -- an overview" a chapter in the book "Computational Intelligence in Automotive Applications" to be published by Springer 2008

[8] E. Ericsson, "Variability in urban driving patterns," Transportation Res. Part D, vol. 5, pp. 337-354, 2000.

[9] E. Ericsson, "Independent driving pattern factors and their influence on fuel-use and exhaust emission factors," Transport. Res. Part D, vol. 6, pp. 325-341, 2001.

[10] Sierra Research," SCF Improvement – Cycle Development," Sierra Report No. SR2003-06-02, 2003.

[11] T. R. Carlson and R. C. Austin, "Development of speed correction cycles," Sierra Research, Inc., Sacramento, CA, Report SR97-04-01, 1997.

[12] PSAT (Power System Analysis Toolkit), http://www.transportation.anl.gov/software/PSAT/index.html

[13] Yi L. Murphey, ZhiHang Chen, Leo Kiliaris, Jungme Park, Ming Kuang, Abul Masrur[3], Anthony Phillips, "Neural Learning of Predicting Driving Environment," Proceedings of International Joint Conference on Neural networks, June, 2008